Molecular Modeling

A Hybrid Solid with Giant Pores Prepared by a Combination of Targeted Chemistry, Simulation, and Powder Diffraction

Gérard Férey, Christian Serre, Caroline Mellot-Draznieks, Franck Millange, Suzy Surblé, Julien Dutour, and Irène Margiolaki*

Molecular gigantism is very topical in inorganic chemistry.[1–5] Inorganic and hybrid nanoporous solids, and keplerates[5] provide illustrations of this trend. Beside its academic interest, this research is motivated by the numerous applications related to this gigantism, such as their use as possible nanoreactors, or in catalysis,[6] gas separation,[7] and gas storage.[8] Besides the systematic chemical search of new systems, two main topological concepts were applied to reach a possible design of porous solids: "scale chemistry"[9] for inorganics and "reticular synthesis from augmented nets"[3,10,11] for metal–organic frameworks (MOFs). These two concepts have however limitations: they cannot always provide polymorphs; their topological predictions rapidly lead to complex structures that are almost impossible to solve in the absence of single crystals. We shall prove in the following that, in the domain of MOFs, the introduction of computer simulation beside targeted chemistry of the inorganic moiety push forward these limits. It leads to a new crystalline MOF (**MIL-100**) with a giant cubic cell, the volume of which is close to 380000 Å^3. It exhibits a hierarchy of micro- ($\varnothing \approx 6.5$ Å) and mesopores ($\varnothing \approx 25$–30 Å) and a large sorption capacity (3100 m^2 g^{-1}).

The dream of the solid-state chemist is the synthesis of "tailor-made" compounds with predicted structures and properties. Forbidden in the case of high-temperature synthesis, which is governed by diffusion processes, the synthesis of tailor-made solids is indeed on the way to being realized in the ever growing domain of MOFs, the synthesis of which gives solids by precipitation of the species from solution. In three main seminal articles,[3,11,12] Yaghi, O'Keeffe, and coworkers progressively defined the concept of reticular chemistry with the chemical and topological rules that govern this possible design. This concept starts from the existence in solution of well defined and rigid inorganic and

[*] G. Férey
Institut universitaire de France
Fax: (+33) 1-3925-4358
E-mail: ferey@chimie.uvsq.fr
G. Férey, C. Serre, C. Mellot-Draznieks, F. Millange, S. Surblé, J. Dutour
Institut Lavoisier
UMR CNRS 8637
Université de Versailles St-Quentin en Yvelines
45 Avenue des Etats-Unis, 78035 Versailles Cedex (France)
I. Margiolaki
ESRF, Grenoble (France)

Supporting information for this article is available on the WWW under http://www.angewandte.org or from the author.

  DOI: 10.1002/ange.200460592

organic building blocks, which must maintain their structural integrity throughout the construction process of the solid. The proper choice of these inorganic and organic building blocks and their assembly by strong bonding must lead to predetermined ordered structures, reminiscent of the topology of dense structures. Numerous examples in the literature illustrate this concept.[9,12]

However, one of the limitations of this approach concerns the enumeration of the possible predetermined frameworks accessible from predefined building blocks. So far, what is usually called "design" is the realization of a reasonable expectation of a given structural arrangement. Indeed, the idea of a framework resulting from the connection of building blocks refers only to the most probable organization, based on an initial intuition strengthened by topological symmetry rules.[12] Keeping in mind the principles of reticular chemistry, we applied our new concept to crystal structures of MOFs with the aim of exploring all possible combinations of connections between inorganic and organic building blocks in the system experimentally under study by using original global optimization simulations.[13] This computational approach takes advantage of our previous AASBU method,[14] based on the concept of secondary building units (SBU), to assemble organic and inorganic units. It explores the whole space of configurations with the corresponding cell parameters, space groups, and theoretical atomic coordinates; it classifies the different solutions by their relative energies and therefore gives the most likely arrangements. The validity of the method was first proved by finding hybrid structures that are already known, built from different types of inorganic and organic building units. Moreover, unknown topologies with reasonable relative "energies" appeared during the calculations for all the inorganic and organic building units considered. Finally, the calculated X-ray powder-diffraction pattern for each candidate topology may be directly compared to patterns obtained experimentally, thus allowing the rapid identification of new phases. The efficiency of this method relates to the way that it is carried out, but requires that the inorganic building block be present at an early stage of the reaction.

We recently developed separately the computational[13] and experimental[15] aspects of our concept. Among the best identified inorganic building blocks, our attention focused on the determination of the chemical conditions leading to trimers that are formed by the assembly of three octahedra sharing a common vertex μ_3-O,[15] because known examples are scarce.[3,16] The conditions used to synthesize the inorganic building units depend on the nature of the cation. Although we initially focused on complexes of Fe^{3+} ions,[15] the search was extended to complexes of Cr^{3+} ions. The combination of Cr^{3+} ions with trimesic acid (benzene-1,3,5-tricarboxylate; BTC) under hydrothermal conditions leads to a new powdered chromium hybrid solid (**MIL-100**).

MIL-100 is a highly crystalline and pure green solid, a chromium trimesate of chemical composition $Cr_3F(H_2O)_3O[C_6H_3\text{-}(CO_2)_3]_2\cdot n\,H_2O$ ($n \sim 28$). Its resulting pattern is so complicated (Figure 1) that, in the absence of single crystals, the knowledge of the related structure is ruled out. Consequently, our new simulation method[13] dedicated to the prediction of MOFs is used to predict candidate crystal structures of **MIL-100**. Candidates polymorphs for the [Cr–BTC] system are simulated as follows. Based on the assumption that there are inorganic trimers (Figure 2a) in the new hybrid **MIL-100**, as highly suggested by our previous results,[15] and that these trimers are linked to the constitutive organic ligand (BTC), possible hybrid building blocks are computationally designed and auto-assembled. Indeed, the arrangement of BTC and inorganic trimers into a large super tetrahedron (ST) was considered as a possible hybrid building block (Figure 2b) and was selected for its compatibility with the chemical composition (metal:organic ratio) of **MIL-100**. The ST is built in such a way that the four vertices of the ST are occupied by the trimers while the organic linker is located at the four faces of the ST. The connection of the ST is established through vertices to ensure a 3D network of "corner-sharing" super tetrahedra. At this stage, three interesting candidates of likely crystal structures were identified and assorted with their full crystallographic parameters together with their simulated X-ray powder patterns. Strikingly, all three candidates are upper homologues of zeotype architectures,[19] that is, MEP, MTN and a new hexagonal type, referred to hereafter as HEX, in which each tetrahedral

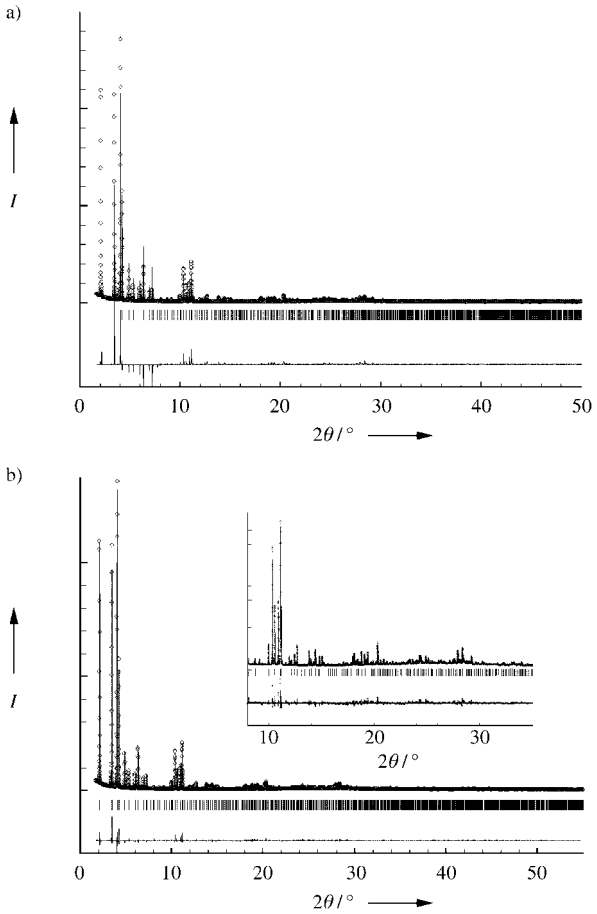

Figure 1. a) Comparison of the simulated X-ray pattern predicted for **MIL-100** (full lines) with that of the experimental (circles). b) Final Rietveld plot of the as-synthesized **MIL-100**. In both figures, the difference spectrum appears at the bottom. I = intensity.

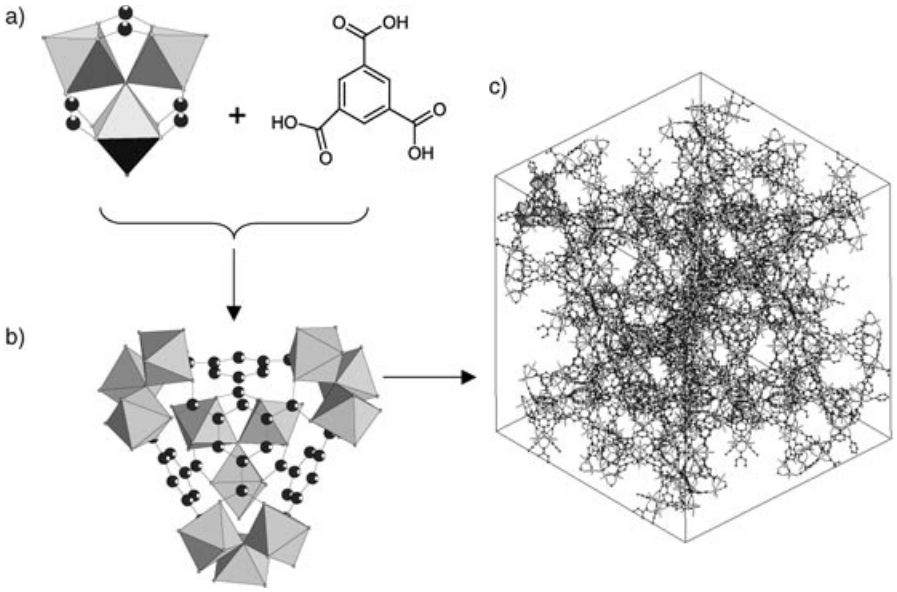

Figure 2. a) The original building block with a trimer of metal octahedra chelated by three carboxylic functions. b) The ST formed by using trimesic acid, which occupies the faces of ST. c) Ball-and-stick view of a unit cell of **MIL-100**; one supertetrahedron is represented by using octahedra for a better understanding. Free water molecules have been omitted for clarity.

center (TO_4), typical of zeolites, is occupied by one super tetrahedron. The corresponding structures, described with more details below (Table 1) illustrate the concept of "scale chemistry".[9] They represent polymorphs with cell volumes in the range 120000–360000 Å^3. Two of them are cubic (MEP, MTN; space group $Fd\bar{3}m$, $Pm\bar{3}n$, respectively), the third is hexagonal (HEX, space group $P6_3/mmc$). From this point of view, our computational approach is able to create the potential upper homologues of numerous silicates and zeolites with ST instead of small tetrahedra.

Interestingly, the simulated pattern of the MTN-type hybrid structure matches the targeted experimental pattern of **MIL-100** (Figure 1 a), thus yielding the solution of the direct-space structure of the new phase and ensuring a valid model for subsequent structure refinement. The diffraction pattern calculated from the MTN-type computed model corresponds exactly to the position of the Bragg peaks of the new structure. The only difference (Figure 1 a) concerns the discrepancy between simulated and experimental intensities; the simulated pattern obtained from the computed model corresponds only to the skeleton whereas the experimental pattern also takes into account the contribution of the occluded species. Owing to the large cell volumes involved, the challenge was then to consider the possibility of a Rietveld refinement of the structure, which required first a very good collection of powder data by using synchrotron radiation (see Experimental Section). Finally, the atomic coordinates and cell parameters of MTN-type model predicted from the simulations were used to perform the Rietveld refinement of the synchrotron diffraction pattern of **MIL-100**. Surprisingly, despite the large number of parameters (67 independent framework atoms, ≈170 parameters, in a cell volume of 387000 Å^3), the refinement converges toward good R values and improves the prediction by locating the position of inserted species, which are free water molecules in the case of **MIL-100**. The final Rietveld plot is represented on Figure 1 b. The refinement correctly converged towards the general formula $Cr_3F(H_2O)_3O[C_6H_3(CO_2)_3]_2{\cdot}nH_2O$ ($n \approx 28$), which is in agreement with the chemical analysis. Extra framework water molecules were localized by using Fourier-difference maps (45 independent water molecules). Full details are given in the Supporting Information.

This is the first time, in the field of hybrid solids, that a rational simulation approach provides a solution of the crystal structure constructed only from topological criteria, which matches the experimental X-ray diffraction pattern of the solid (Figure 1). It is a new method in which conventional direct- or reciprocal-space methods cannot be used in the structure-solution process. The very-

Table 1: Simulation of Cr–BTC hybrid frameworks: Selected structural features of three candidate polymorphs.

[a] *MTN*		
cubic $Fd\bar{3}m$	BTC	
a [Å]	71.26	
V [Å^3]	361774	
No. of independent positions per asymmetric unit	68	
$Density_{calcd}$ [g cm^{-3}][b]	0.7843	
Supertetrahedron		
Edge length [Å] (between μ_3O)	9.40	
No. of atoms of the wall	24 $O_{carboxy}$ + 36 C_{BTC} + 12 M	
Internal diameter [Å]	6.64	
(Recall for C_{84}: 18.96–2.80 = 16.16 Å)		
Pentagonododecahedral cages (20 vertices)		
Coordinates of the centroid	0,0,0 (16*c* positions of $Fd\bar{3}m$ with origin at 0,0,0)	
Accessible diameter [Å]	24.6	with R_c^{vdw}: 1.40 Å
Large cages (28 vertices)		
Coordinates of the centroid	1/8,1/8,1/8 (8*a* positions of $Fd\bar{3}m$ with origin at 0,0,0)	
Accessible diameter [Å]	31.0	with R_c^{vdw}: 1.40 Å
[a] *MEP*		
cubic $Pm\bar{3}n$	BTC	
a [Å]	49.27	
V [Å^3]	119635	
No. of independent positions per asymmetric unit	82	
$Density_{calcd}$ [g cm^{-3}][b]	0.8022	

Table 1: (Continued)

Supertetrahedron		
Edge length [Å] (between μ_3O)	9.40	
No. of atoms of the wall	24 $O_{carboxy}$ + 36 C_{BTC} + 12 M	
Internal diameter [Å]	6.64	with R_c^{vdw}:1.40 Å
Pentagonododecahedral cages (20 vertices)		
Coordinates of the centroid	0,0,0 (2a positions of $Pm\bar{3}n$ with origin at 0,0,0)	
Accessible diameter [Å]	24.5	with R_c^{vdw}:1.40 Å
Large cages (24 vertices; ovoidal)		
Coordinates of the centroid	1/2,0,3/4 (12f positions of $Pm\bar{3}n$ with origin at 0,0,0)	
Accessible diameter [Å]	29.2–20.2	with R_c^{vdw}:1.40 Å
[a]NEW HEX		
hexagonal $P6_3/mmc$	BTC	
a [Å]	50.17	
c [Å]	82.12	
V [Å^3]	179179	
No. of independent positions per asymmetric unit	245	
$Density_{calcd}$ [g cm^{-3}][b]	0.7918	
Supertetrahedron		
Edge length [Å] (between μ_3O)	9.40	
No. of atoms of the wall	24 $O_{carboxy}$ + 36 C_{BTC} + 12 M	
Internal diameter [Å]	6.64	with R_c^{vdw}:1.40 Å
Pentagonododecahedral cages (20 vertices)		
Coordinates of the centroid	0.8495, 0.1701, 0.2439 (24l positions of $P6_3/mmc$ (194) with origin at 0,0,0)	
Accessible diameter [Å]	25	with R_c^{vdw}:1.40 Å
Large cages (28 vertices)		
Coordinates of the centroid	1/3,2/3,0.40 (4f positions of $P6_3/mmc$ (194) with origin at 0,0,0)	
Accessible diameter [Å]	29.7	with R_c^{vdw}:1.40 Å

[a] MTN, MEP refer to a zeolitic structure type (see Atlas of Zeolites, http://www.iza-structure.org/); NEW HEX does not correspond to any known structural type. [b] Densities are estimated by using the Cr form of the simulated topologies.

large cell volume involved in our results opens the window to the discovery of numerous new solids with huge potential applications. In the absence of single crystals, such solids could never be tackled before owing to the extreme complexity of the corresponding structures. They now become accessible.

In the supertetrahedra (see Supporting Information), all the bond lengths are in the usual range (1.81–2.18 Å for Cr–O, 1.37–1.64 Å for C–C; 1.23–1.37 Å for C–O). Moreover, valence-bond calculations show that in the trimer the terminal oxygen atom is from a water molecule. The aromatic ring of BTC occupies the center of the faces of the ST. Within the ST, the cage, which has 24 oxygen atoms and carbon 36 atoms and an internal diameter of 6.6 Å. This dimension corresponds to the domain of micropores, in the same range as zeolites.

More interestingly, the corner sharing of the ST delimits a framework with two types of cages (Figure 3), whose dimensions are now typically in the range of mesopores. The smallest cage, which has 20 ST, has an internal diameter of $\approx$25 Å. The polyhedron obtained by joining the centers of the ST is a pentagon dodecahedron (the free opening of the pentagonal windows: ($\approx 4.8 \times 5.8$ Å) being rather small because the terminal water molecules of the trimer point toward the center of the window). The centers of the dodecahedra, are in the (0,0,0) 16c positions of the space group $Fd\bar{3}m$ (origin choice 2). The subnetwork that joins these centers forms corner-linked tetrahedra as in the pyrochlore structure.[17] The dodecahedra share faces and form (see the Supporting Information) infinite linear rodlike chains,[18] which cross orthogonally to each other through common faces to ensure the 3D network. This connection creates larger cavities, which have 28 ST. These cages are centered on the (1/8,1/8,1/8) 8a sites of the space group $Fd\bar{3}m$. The polyhedron determined by the centers of the ST has now 12 pentagonal and 4 hexagonal faces. The aperture of the large hexagonal windows is $\approx 8.6 \times 8.6$ Å^2 and the internal diameter becomes close to $\approx$29 Å. In the as-prepared materials, the cavities are occupied only by water molecules. The location of the fluoride counterions within **MIL-100** could not be determined due to the similar diffusion factors of oxygen and fluorine atoms; thus, these anions may be either located in terminal position bound to chromium atoms or within cages as they are in previous structures based on iron trimers.[15]

In inorganic chemistry, such dimensions of pores are mostly reached with mesoporous solids, which, in contrast to the compounds presented herein, have amorphous walls. Thus, **MIL-100** provides the first example of a porous solid with crystalline walls, with a unique hierarchical system of three types of cages of different dimensions. Indeed, this solid may have applications in the domain of adsorption/separation of species.

The two other polymorphs found by our computer simulations have the same relative "energy" cost as **MIL-100** (see Table 1). Both of them have infinite chains of face sharing pentagon dodecahedral cages, already described for **MIL-100**. In the cubic structure ($Pm\bar{3}n$), the corresponding rods cross in three directions of space, thus creating larger cages, this time with 24 vertices instead of 28 and the resulting framework is an upper homologue of zeolite MEP.[19] The topology of the hexagonal polymorph ($P6_3/mmc$), hitherto

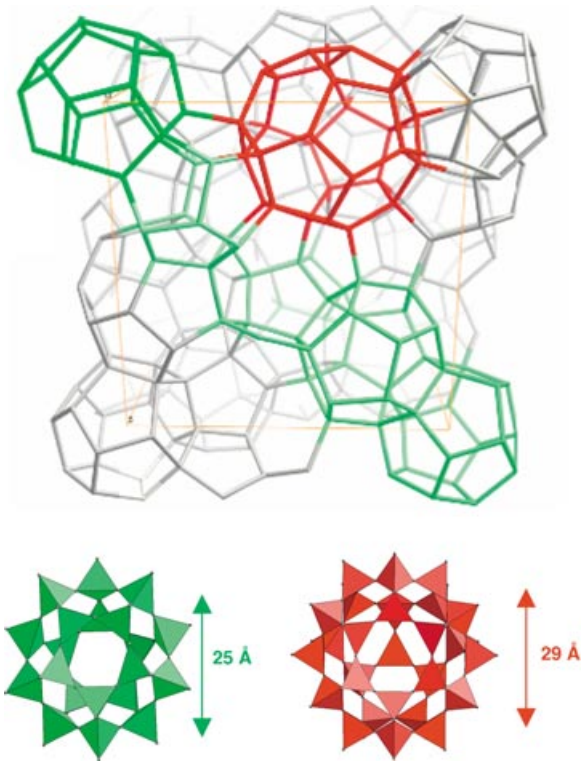

Figure 3. Top: Schematic view of the 3D organization of the structure of **MIL-100** with the medium (green) and large (red) cages delimited by the vertex sharing of the ST (the vertices represent the centers of each ST). Bottom: View and dimensions of the two different cages (green, 20 tetrahedra; red, 28 tetrahedra). The medium cages share faces and form interconnected rods (in green) in the interstices of which are located the large cages.

unknown, corresponds to intersecting rods at 60° to each other, and the larger cages are the same as those in **MIL-100**.

The thermal behavior and the sorption properties of **MIL-100** were investigated. First, the thermal gravimetric analysis carried out in air (see Supporting Information) reveals an interesting stability of the title phase up to 275 °C. X-ray thermodiffractometry shows that the evacuation of the guests does not affect the topology of the skeleton; only the intensity of some Bragg peaks change, otherwise the pattern fits with that predicted. Second, the title material takes up gases readily. The gaseous N_2 sorption isotherm on the fully evacuated samples (Figure 4) is between type I and IV with a slight secondary uptake, which is indicative of the presence of both micro- and mesopores. No hysteresis is observed. Using the Dubinin-Raduskhvich equation, we found a pore volume of around 1.16 $cm^3 g^{-1}$ for **MIL-100**. For a monolayer coverage of N_2 (which may not be strictly correct with such large cavities), we estimate the apparent Langmuir surface area to be 3100(40) $m^2 g^{-1}$, which is close to the highest values known.[20]

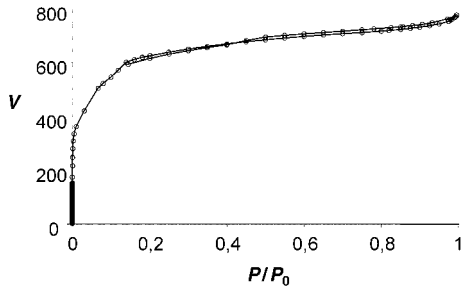

Figure 4. Nitrogen gas sorption isotherm at 78 K for MIL-100 degased overnight at 100 °C. P/P_0 is the ratio of gas pressure (P) to saturation pressure (P_0 = 750 torr). V is the adsorbed volume ($cm^3 g^{-1}$).

In conclusion, we have shown from a straightforward example the strength of the combined chemistry–simulation approach for obtaining new materials. The resulting hybrid chromium carboxylate, **MIL-100**, has an eye-catching structure that has a hierarchical pore system (micro: ≈5–9 Å; mesoporous: ≈25–30 Å) with a very-high surface area (≈3100 $m^2 g^{-1}$). While tackling the polymorphism of MOFs by limiting the domain of structures that are possible for a given metal–organic ligand pair, we found that simulations applied to hybrids is a tangible route towards structure solution in direct space. This new approach has the advantage that single crystals are not required for the resolution of the structures, which can be done from Rietveld refinements of powder-diffraction data. This represents a useful tool to bridge a gap because many solids, previously isolated by several groups, were abandoned owing to the lack of single crystals and the complexity of the powder patterns. Incidentally, the results obtained here open a window of opportunity to search for new porous solids with giant pores, which represent the upper homologues of numerous well-known zeolites. This work provides a new example of the possibilities of the concept of "scale chemistry": the increase of the size of the ST generates larger pores, which open the way to new applications for MOF porous solids. Finally, the question may be posed as to whether structures such as **MIL-100** arise from design. The answer is clearly no because in design, one must first imagine something then realize it afterwards. In our approach, the first step does not involve imagination (which is a creative act), but is the result of a computational prediction. For this reason, we prefer to suggest that the label of "simulation assisted chemical structures" (SACS) is the best description for solids obtained by using our method.

Experimental Section

Syntheses and chemical analyses: Metallic chromium (52 mg, 1 mmol; Aldrich, 99%) was dispersed into an aqueous solution of 5 M hydrofluoric acid (0.4 mL, 2 mmol). After the addition of 1,3,5-benzene tricarboxylic acid H_3BTC (150 mg, 0.67 mmol; Aldrich, 99%) and H_2O (4.8 mL, 265×10^{-3} mol), the mixture was heated in a hydrothermal bomb at a rate of 20.0 °C h^{-1} to 220 °C, kept at this temperature during 96 h, then cooled at a rate of 10.0 °C h^{-1} to room temperature. The resulting green powder was washed with deionized water and acetone and dried in air. The yield of the reaction was ≈45% based on chromium.

Chemical analyses: These were performed at the National Center of Analysis of the CNRS in Vernaison (France). As the amount of water present in the samples is very sensitive to the temperature (see TGA), only the C:Cr and F:Cr ratios are significant. They agree well with the formula deduced from the structure ($C:Cr_{exp}$ calcd 6.0, found 6.75; F:Cr calcd 0.33, found 0.31).

TGA measurements: A crystalline sample was heated from 25 to 600 °C in air at a constant rate of 2 °C min^{-1}. Two weight-loss steps

were observed: the first (35% of initial weight) occurred between 25 and 250°C and is attributed to the loss of guest water molecules (calcd 40%); the second (44% of initial weight) is due to the removal of fluoride ions and the decomposition of the framework and occurred between 275 and 400°C.

Sorption measurements: Experiments were performed on a Micromeritics ASAP 2010 with nitrogen as the adsorbed gas. **MIL-100** was dehydrated under vacuum overnight at 150°C.

Crystallographic study: Powder X-ray diffraction data were collected at the high resolution beamline ID31 of the European Synchrotron radiation Source (ESRF), Grenoble (France), from a sample contained in a 1 mm diameter capillary. ID31 beamline receives X-rays from the synchrotron source (which operates with an average energy of 6 GeV and a current beam of typically 200 mA) from an ondulator device. The incident X-ray wavelength was 1.55075 Å. Data collection was performed over the angular range 1–97° 2Θ, with a step 0.005° at 80 K by using a cryostream (cold nitrogen gas blower). Cubic cell, $a = 72.906$ Å (**MIL-100**) with adequate figures of merit was found. Systematic absences were consistent with the space group $Fd\bar{3}m$ (no. 227). After the pattern had been matched, the structure refinement was initiated by using the atomic positions obtained from the simulations. The final agreement factors (Figure 1b) were satisfactory: $R_p = 5.48\%$, $R_{wp} = 7.61\%$, and $R_{Bragg} = 9.28\%$. For details see the Supporting Information.

The Supporting Information accompanying this paper contains crystallographic and TGA data.

Received: May 7, 2004

Keywords: microporous materials · molecular modeling · nanoporous materials · organic–inorganic hybrid composites · powder diffraction

[1] G. Férey, A. K. Cheetham, *Science* **1999**, *283*, 1125 – 1126; G. Férey, *Science* **2000**, *289*, 994 – 995.
[2] H. Li, M. Eddaoudi, M. O'Keeffe, O. M. Yaghi, *Nature* **1999**, *402*, 276 – 279.
[3] O. M. Yaghi, M. O'Keeffe, N. W. Ockwig, H. K. Chae, M. Eddaoudi, J. Kim, *Nature* **2003**, *423*, 705 – 714; M. Eddaoudi, J. Kim, N. Rosi, D. Vodak, J. Wachter, M. O'Keeffe, O. M. Yaghi, *Science* **2002**, *295*, 469 – 472.
[4] L. Beitone, C. Huguenard, M. Henry, F. Taulelle, T. Loiseau, G. Férey, *J. Am. Chem. Soc.* **2003**, *125*, 9102 – 9110.
[5] A. Müller, E. Krickemeyer, H. Bögge, M. Schmidtmann, S. Roy, A. Berkle, *Angew. Chem.* **2002**, *114*, 3756 – 3761; *Angew. Chem. Int. Ed.* **2002**, *41*, 3604 – 3609; A. Müller, S. K. Das, S. Talismanov, S. Roy, E. Beckmann, H. Bögge, M. Schmidtmann, A. Merca, A. Berkle, L. Allouche, Y. Zhou, L. Zhang, *Angew. Chem.* **2003**, *115*, 5193 – 5198; *Angew. Chem. Int. Ed.* **2003**, *42*, 5039 – 5044.
[6] N. Guillou, P. M. Forster, Q. Gao, J. S. Chang, M. Nogues, S.-E. Park, A. K. Cheetham, G. Férey, *Angew. Chem.* **2001**, *113*, 2913 – 2916; *Angew. Chem. Int. Ed.* **2001**, *40*, 2831 – 2834.
[7] F. Schüth, K. S. W. Sing in *Handbook of Porous Solids* (Eds.: J. Weitkamp), Wiley-VCH, Weinheim, **2002**.
[8] S. Kitagawa, M. Kondo, *Bull. Chem. Soc. Jpn.* **1998**, *71*, 1739 – 1753; P. M. Forster, J. Eckert, J.-S. Chang, S.-E. Park, G. Férey, A. K. Cheetham, *J. Am. Chem. Soc.* **2003**, *125*, 1309 – 1312; N. Rosi, J. Eckert, M. Eddaoudi, D. Vodak, J. Kim, M. O'Keeffe, O. M. Yaghi, *Science* **2003**, *300*, 1127 – 1129; G. Férey, M. Latroche, C. Serre, F. Millange, T. Loiseau, A. Percheron-Guégan, *Chem. Commun.* **2003**, 2276.
[9] G. Férey, *J. Solid State Chem.* **2000**, *152*, 37 – 48; G. Férey, *J. Solid State Sci.* **2003**, *5*, 79 – 94.
[10] O. M. Yaghi, M. O'Keeffe, M. Kanatzidis, *J. Solid State Chem.* **2000**, *152*, 1 – 321.
[11] M. Eddaoudi, D. B. Moler, H. Li, B. Chen, T. M. Reineke, M. O'Keeffe, O. M. Yaghi, *Acc. Chem. Res.* **2001**, *34*, 319 – 330.
[12] O. Delgado-Friedrichs, M. O'Keeffe, O. M. Yaghi, *Acta Crystallogr. Sect. A* **2003**, *59*, 22 – 27.
[13] C. Mellot-Draznieks, J. Dutour, G. Férey, *Angew. Chem.* **2004**, *116*, 6450–6456; *Angew. Chem. Int. Ed.* **2004**, *43*, 6290–6296.
[14] C. Mellot-Draznieks, J. M. Newsam, A. M. Gorman, C. M. Freeman, G. Férey, *Angew. Chem.* **2000**, *112*, 2258 – 2363; *Angew. Chem. Int. Ed.* **2000**, *39*, 2270 – 2275; C. Mellot-Draznieks, S. Girard, G. Férey, C. Schön, Z. Cancarevic, M. Jansen, *Chem. Eur. J.* **2002**, *8*, 4103 – 4113; C. Mellot-Draznieks, S. Girard, G. Férey, *J. Am. Chem. Soc.* **2002**, *124*, 15326 – 15335.
[15] C. Serre, F. Millange, S. Surblé, G. Férey, *Angew. Chem.* **2004**, *116*, 6445–6449; *Angew. Chem. Int. Ed.* **2004**, *43*, 6285–6289.
[16] J. S. Seo, D. Wang, H. Lee, S. I. Jun, J. Oh, Y. J. Jeon, K. Kim, *Nature* **2000**, *404*, 982 – 986.
[17] R. De Pape, G. Férey, *Mater. Res. Bull.* **1986**, *21*, 971 – 978.
[18] M. O'Keeffe, S. Andersson, *Acta Crystallogr. Sect. A* **1977**, *33*, 914 – 923; S. Lidin, M. Jacob, S. Andersson, *J. Solid State Chem.* **1995**, *114*, 36 – 41.
[19] M. M. J. Treacy, J. B. Higgins in *Collection of Simulated XRD Powder Patterns for Zeolites*, *4th ed.*, Elsevier **2001**, and http://www.iza-structure.org/databases/.
[20] H. K. Chae, D. Y. Siberio-Perez, J. Kim, Y.-B. Go, M. Eddaoudi, A. J. Matzger, M. O'Keeffe, O. M. Yaghi, *Nature* **2004**, *427*, 523 – 527.

